Depression Uncouples Brain Hate Circuit

Haojuan Tao[1,#], Shuixia Guo[2,#], Tian Ge[3,#], Keith M. Kendrick[4,#],

Zhimin Xue[1], Zhening Liu[1,*], Jianfeng Feng[3,5,*]

[1]Institute of Mental Health, Second Xiangya Hospital, Central South University, Changsha 410011, PR China;

[2]Mathematics and Computer Science College, Hunan Normal University, Changsha 410081, PR China;

[3]Centre for Computational Systems Biology, School of Mathematical Sciences, Fudan University, Shanghai 200433, PR China;

[4]Cognitive and Systems Neuroscience Group, The Babraham Institute, Cambridge CB22 3AT, UK;

[5]Department of Computer Science, University of Warwick, Coventry CV4 7AL, UK.

[#]These authors contributed equally to this work.

*Correspondence should be addressed to

Jianfeng Feng, email: jianfeng64@gmail.com

Zhening Liu, email: zningl@163.com

ABSTRACT

It is increasingly recognized that we need a better understanding of how mental disorders such as depression alter the brain's functional connections to improve both early diagnosis and therapy. A new holistic approach has been used to investigate functional connectivity changes in the brains of patients suffering from major depression using resting state fMRI data. A canonical template of connectivity in 90 different brain regions was constructed from healthy control subjects and this identified a six-community structure with each network corresponding to a different functional system. This template was compared to functional networks derived from fMRI scans of both first episode and longer-term, drug resistant, patients suffering from severe depression. The greatest change in both groups of depressed patients was uncoupling of the so-called "hate circuit" involving the superior frontal gyrus, insula and putamen. Other major changes occurred in circuits related to risk and action responses, reward and emotion, attention and memory processing. A voxel-based morphometry analysis was also carried out but this revealed no evidence in the depressed patients for altered grey or white matter densities in the regions showing altered functional connectivity. This is the first evidence for involvement of the "hate circuit" in depression and suggests a potential reappraisal of the key neural circuitry involved. We have hypothesized that this may reflect reduced cognitive control over negative feelings towards both self and others.

Key words: mental disorder, major depression, fMRI, functional connectivity, hate circuit, voxel-based morphometry.

INTRODUCTION

At the brain circuit level, most of what we understand about depression and its biological abnormalities during the resting state comes from fMRI studies targeting changes in a small number of brain regions, as recently reviewed in (1, 2). These studies have suggested the involvement of a default mode network including the dorsal anterior cingulate cortex and some subcortical areas such as amygdala and thalamus (3-7). However, the conclusions drawn from these studies are based on either seed-based analysis or independent component analysis (ICA) and are questionable in spite of the wide and successful application of such methods in the analysis of resting state fMRI data (8-13). Seed-based analysis is a hypothesis-driven approach which means the foci (seeds) of the disorder must be specified a priori. It is therefore a biased approach lacking a global and independent view (14). With the ICA approach it is assumed that the human brain is composed of independent components whereas in reality different parts of the human brain undoubtedly work in a coordinated fashion. Hence, given the complexity and multiple causes of depression together with variability between individuals, a novel, unbiased approach is urgently called for which identifies pathway changes in a holistic manner.

In the current paper, we have adopted such a new holistic approach aiming to unambiguously identify the key connections which are modified in the brains of depressed patients. To achieve this we have first ap-

plied a canonical template constructed for the whole brain based upon data from a large number of healthy individuals. Using a community of discovery algorithms we have developed previously (15), six discrete interconnected communities were recovered from this template, each corresponding to a functional system in the human brain: a default mode network which has been reported extensively in the literature (11, 12), an attention network consisting of frontal and parietal areas, the auditory system, the visual system, the sensory-motor areas and finally a subcortical network. Corresponding functional maps for patients suffering from severe depression with or without pharmacological treatments (first-episode major depressive disorder (FEMDD) patients and resistant major depressive disorder (RMDD) patients) were then constructed using a similar approach enabling us to carry out a thorough comparison between the brains of healthy and depressed individuals. Voxel-based morphometry analysis was also carried out to assess whether gray or white matter volume changes occurred in those brain regions of depressed patients showing altered functional connectivity.

The most significant differences between both FEMDD and RMDD patients and healthy populations occurred in inter-community rather than intra-community links. The greatest change was in a circuit associated with feelings of hate, comprising the superior frontal gyrus, insula and putamen (16), where these regions were uncoupled in depressed patients

in both hemispheres. The other main circuits identified which were significantly affected in depressed patients included those involved with risk-taking and action, emotion and reward, attention and memory. This is the first time changes in the functional connectivity of the so called "hate circuit" have been identified in the brains of depressed patients.

METHODS

Subjects Fifteen treatment-naive adult patients with first-episode major depressive disorder (FEMDD) (7 females, 8 males; mean age 28.27 +/- 7.45 years old; mean education 12.13 +/- 3.60 years) and twenty four treatment-resistant major depressive disorder (RMDD) patients (16 females, 8 males; mean age 27.83 +/- 7.86 years old; mean education 11.92 +/- 3.56 years) were recruited from inpatient or outpatient departments of the Second Xiangya Hospital of Central South University in Changsha, Hunan province, China. The mean illness duration for patients with FEMDD was 21.10 +/- 24.67 months, and the mean score on the 17-item version of Hamilton Rating Scale for Depression (HAMD) (17, 18) was 26.07 +/- 6.51. The mean illness duration for patients with RMDD was 34.00 +/- 45.14 months, and the mean score on the 17-item version of Hamilton Rating Scale for Depression (HAMD) was 24.29 +/- 3.70. None of the patients had co-morbidities with other disorders. Detailed treatments for RMDD patients can be found in Supplementary Table S1.

All RMDD patients were taking antidepressants at the time of the MRI scan and treatment resistance was defined as non-responsiveness to at least two adequate trials in terms of dosage, duration (6 weeks for each trial), and use of different classes of antidepressants consistent with previous studies (19, 20). Non-responsiveness was defined as a less than 50% reduction in HRSD score (21) after a treatment at a minimum dose of 150 mg/day of imipramine equivalents (dose converted using a conversion table (22)) for 6 weeks.

Thirty seven age, gender and education duration matched healthy control subjects (14 females, 23 males; mean age 28.22 +/- 6.47 years old; mean education 13.32 +/- 3.29 years) were also recruited (gender matching: chi-square test, $\chi^2 = 4.873$, $p = 0.087$; age matching: $F = 0.037$, $p = 0.964$ and education matching: $F = 1.205$, $p = 0.306$).

All patients met the following inclusion criteria: (I) Current MDD attack as assessed by two experienced psychiatrists using the Structural Clinical Interview for DSM-IV; (II) 18 to 45 years of age; (III) Right-handed Han Chinese; (IV) HAMD scores of at least 17; (V) Treatment-naive adult patients with FEMDD had not taken any medication before MRI scan.

Patients and healthy controls were excluded if they had any of the following: (I) A history of neurological diseases or other serious physical diseases; (II) A history of electroconvulsive therapy; (III) History of sub-

stance (i.e. drugs, alcohol and other psychoactive substance) abuse; (IV) Co-morbidities with other disorders (no evidence for schizoaffective disorder or Axis II, personality disorders and mental retardation); (V) Any contraindications for MRI.

This study was approved by the Ethics Committee of the Second Xiangya Hospital, Central South University, Hunan, China. Written informed consent was obtained from all subjects.

Imaging acquisitions and data preprocessing All functional imaging data were acquired using a 1.5T GE Signa Twinspeed scanner (General Electric Medical System, Milwaukee, Wisconsin) at the Second Xiangya Hospital of Central South University in Changsha, Hunan Province, China. A total of 180 volumes of EPI images were obtained axially (repetition time, 2000ms; echo time, 40ms; slices, 20; thickness, 5mm; gap, 1mm; field of view (FOV), 24 x 24 mm^2; resolution, 64 x 64; flip angle, 90 degrees.)

Prior to functional images preprocessing, the first 10 volumes were discarded to allow for scanner stabilization and the subjects' adaptation to the environment. fMRI data preprocessing was then conducted by SPM8 (*http://www.fil.ion.ucl.ac.uk/spm*) and a Data Processing Assistant for Resting-State fMRI (DPARSF) (23). Briefly, the remaining functional scans were first corrected for within-scan acquisition time differences

between slices, and then realigned to the middle volume to correct for inter-scan head motions. Subsequently, the functional scans were spatially normalized to a standard template (Montreal Neurological Institute) and resampled to 3 x 3 x 3mm^3. After normalization, the BOLD signal of each voxel was firstly detrended to abandon linear trend and then passed through a band-pass filter (0.01 – 0.08Hz) to reduce low-frequency drift and high frequency physiological noise. Finally, nuisance covariates including head motion parameters, global mean signals, white matter signals and cerebrospinal fluid signals were regressed out from the BOLD signals.

High-resolution whole brain volume T1-weighted images were acquired sagittally with a 3D spoiled gradient echo (SPGR) pulse sequence (repetition time, 12.1ms; echo time, 4.2ms; flip angle, 15 degree; field of view= 240 x 240mm; acquisition matrix, 256 x 256; thickness, 1.8 mm; number of excitations, 2; 172 slices.) All T1-weighted structural data were processed with VBM5 toolbox (*http://dbm.neuro.unijena.de/vbm*) based on the SPM software package. After modulate normalizing, the images were segmented into grey matter, white matter and the cerebrospinal fluid. These segmented images were smoothed using a 12 mm FWHM Gaussian kernel. An automated anatomical labeling (AAL) atlas (24) was used to parcellate the brain into 90 regions of interest (ROIs) (45 in each hemisphere). The names of the ROIs and their corresponding ab-

breviations are listed in Table 1. Volumes of the grey matter and the white matter for each ROI were extracted. Two sample t-tests with Bonferroni correction were then used to assess whether there were significant volume differences between patients and normal controls.

Construction of whole-brain functional network After data preprocessing, the time series were extracted in each ROI by averaging the signals of all voxels within that region. Pearson correlation coefficients between all pairs of ROIs were first calculated. Significant correlations were detected with a p value smaller than 0.01. A 90 x 90 correlation matrix was obtained for each subject. However, significant correlation between two ROIs may be spurious, i.e. a by-product of the correlations of the two ROIs with a third region. To find out whether the correlation for the two ROIs is genuine, the third ROI should be kept constant. Statistically, this problem can be tackled by means of a partial correlation test. In such a test, the effects of the third ROI upon the relation between the other two ROIs are eliminated. By calculating partial correlation coefficients between all pairs of ROIs with all the remaining ROIs being controlling variables, a 90 x 90 correlation matrix was obtained for each subject with a p value smaller than 0.01. The population level network can be obtained by summarizing all individual networks in FEMDD, RMDD and Healthy subject groups respectively and thresholding them into binarized matrices

with matched and reasonable sparsity values (defined as the total number of edges in a network divided by the maximum number of possible edges). In the analysis of this paper, the sparsities of the normal, FEMDD and RMDD networks were 2.74%, 2.77% and 2.64% respectively.

Community mining algorithm A network community generally refers to a group of vertices within which the connecting links are dense but sparse in between. In this study, a community structure of the functional network of the brain corresponds to groups of brain regions that have similar functions and dense functional connectivity with each other. Our former developed community mining algorithm described in (15) tries to explore the notion of network modularity by means of understanding the dynamics of the network, which can naturally reflect the intrinsic properties of the network with modularity structure and exhibit local mixing behaviors. Based on large deviation theory (15), this algorithm sheds light on the fundamental significance of the network communities and the intrinsic relationships between the modularity and the characteristics of the network. See Supplementary Information for more details.

RESULTS

Canonical template The six-community structure constructed for the whole brain from 37 healthy subjects is shown in Fig. 1a. Each dot

represents a significant link between two brain regions, with their names listed in Table 1. For clarity, only one dot is plotted for any two linked regions and it is easy to see the existence of the six communities in the whole brain. We have observed this same structure in an even larger population of around 400 people (data from Cambridge USA and Beijing publicly available in (25), results not shown). Fig. 1b is the actual correlation matrix for a randomly selected individual, showing again the clear community structure. The six communities correspond to six Resting State Networks (RSN) which can be identified in terms of broad functions and can be classified as a default mode network (DMN) (RSN1), an attention network (RSN2), a visual recognition network (RSN3), an auditory network (RSN4), sensory-motor areas (RSN5) and a subcortical network (RSN6). Fig. 1c shows the medial and lateral views of the cortical surface mapping of the six-community structure.

FEMDD and RMDD patients For both the 15 FEMDD patients and 24 RMDD patients, functional maps were constructed and compared with those for the healthy subject group. Comparing the FEMDD network with the canonical template from healthy subjects, there are 97 common links which appear in both networks, 14 links which appear in healthy subjects but are absent in the FEMDD network and 15 links which appear in the FEMDD network but cannot be found in the canonical template.

For the RMDD and healthy subject networks, there are 93 common links, 14 links which only appear in the RMDD network and 18 links which appear in the healthy subjects only. In order to rank the significance of the change for each link, a score is defined as follows for each particular link:

$$S = \frac{L_h}{N_h} - \frac{L_p}{N_p}$$

where s is the score for a particular link, L_p is the number of this link present in the individual networks of depressives, N_p is the total number of patients, L_h is the number of this link present in the individual networks of normal controls, and N_h is the total number of healthy controls. Scores for different links in the two hemispheres between the FEMDD network and the canonical template are shown in Fig. 2a and those between the RMDD network and canonical template in Fig. 2b. The summations of the scores for links within each resting state network (RSN) in both FEMDD and RMDD networks are shown in Fig. 2c. To better visualize the changes, Figs. 3a and b show the altered connections for the two patient groups but without differentiating between brain hemispheres. Scores for the links altered in both hemispheres are combined to aid clarity. Figs. 4a and b do the same but to illustrate similarities and differences between changes in the two patient groups. It can be seen from these figures that the strongest evidence for reduced connectivity compared with control subjects in both FEMDD and RMDD is that between the insula

and putamen in both brain hemispheres (*s*=0.4 and 0.25 for FEMDD and RMDD respectively). Additionally, the link between the left superior frontal gyrus and the right insula is also reduced (*s*= 0.2991 and 0.2658). Thus links between the three main components of the "hate circuit" have become largely uncoupled. Connections to the left inferior frontal gyrus (opercular) from the left precentral gyrus (*s*=0.0991 and 0.0574) and those from the right inferior frontal gyrus (opercular) to the right supramarginal gyrus (*s*=0.0991 and 0.1824) are also reduced together with those from left precentral gyrus to the left inferior parietal lobe (*s*=0.1261 and 0.0845). These four regions comprise a risk/action circuit. In what we have designated as an emotion/reward circuit, the connection from the superior to the inferior orbitofrontal cortex, is considerably weakened in the left hemisphere of depressed patients (*s*=0.3532 and 0.2782) but correspondingly strengthened in the right hemisphere (*s*=-0.1423 and -0.259). There is also a weakening of the connection between the right lingual gyrus and right fusiform gyrus in the visual recognition circuit (*s*=0.0991 and 0.0991) and between the right angular gyrus and right precuneus in the default circuit (*s*=0.2324 and 0.0158). In both groups of depressed patients strengthened connections were also found within a number of circuits, most notably between the left hippocampus and right parahippocampal gyrus in the subcortical network (*s*=-0.2505 and -0.3255) but also between the right inferior frontal gyrus (triangular) and right inferior or-

bitofrontal cortex (*s*=-0.1279 and -0.2196) and between the right medial frontal gyrus and right inferior frontal gyrus (triangular) (*s*=0.1658 and 0.3074) in the attention circuit. Finally, the connection between the right cuneus and left superior occipital gyrus in the visual recognition circuit (*s*=-0.1946 and -0.0529) was strengthened.

With the large number of individual connections analyzed between 90 different brain structures, the changes for individual links could fail to be significant after making corrections for multiple comparisons. We therefore also carried out a permutation analysis on total scores for different circuits (the summation of the scores for all altered links within a circuit) to assess significance of changes in depressed patients. A comparison of the total scores for the main inter-community connection changes was 0.61 ($p = 0.003$) for the hate circuit (superior frontal gyrus, insula and putamen), 0.32 ($p = 0.026$) for the risk/action circuit (inferior frontal gyrus (opercular), precentral gyrus, superior medial gyrus and inferior parietal lobule) and 0.52 (p=1.76e-4) for the emotion/reward circuit (superior and medial orbitofrontal cortex). The main intra-community circuit changes were in the attentional circuit (right inferior frontal gyrus (triangular), right inferior orbitofrontal cortex and medial frontal gyrus) (*s*=0.4, $p = 0.007$) and between the hippocampus and parahippocampal gyrus (*s*=0.29, $p = 0.005$). The overall change in the visual circuit (cuneus, superior occipital gyrus, angular gyrus and fusiform gyrus) just failed to

achieve significance (s=0.23, p = 0.06).

Voxel-based morphometry analysis revealed no significant ($p > 0.05$ t-test with Bonferroni correction) grey or white matter volume reductions in these pathways. (See Supplementary Tables S2-4 for details of the grey/white matter volumes of the ROIs involved in these pathways for both patients and normal controls are listed.

DISCUSSION

The holistic approach adopted here to identify altered functional circuits in the brains of depressed patients has proved to be very informative. The approach is completely different from existing methods: seed-based analysis and independent component analysis - and makes no assumptions about which circuits might be altered or that brain regions are independent of one another. Furthermore, our approach has identified the so called “hate circuit”, as the one showing the largest change in both FEMDD and RMDD, although similar major changes also occurred in the emotion and risk/action circuits. This involvement of the “hate circuit” has not, to the best of our knowledge, been found in previous studies. Interestingly, some of the main circuitry identified by other studies using an a priori seed-based approach, such as the links related to the amygdala and cingulate cortex (4-7), was not found to be altered consistently in both patient groups. A link with the amygdala was present in RMDD, but

absent in FEMDD, while the cingulate link was absent in RMDD but present in FEMDD.

Overall our voxel-based morphometry analysis revealed no significant grey or white matter changes in any of the brain regions showing connectivity changes in depressed patients. It therefore seems unlikely that observed changes were simply caused by reduced tissue volumes.

Although the current approach has only been applied to one of the major brain disorders, depression, it is clear that it could be easily applied to other forms of psychiatric, developmental or neurodegenerative disorders and provide information on how each of these disorders are characterized by a specific subset of functional connectivity changes as well as helping to identify possible common traits across, for example, affective or learning and memory disorders.

It could be argued that the changes in functional circuit we have identified are simply a reflection of altered coherent activities (both positive and negative correlations) among brain regions in the resting state and that they might not be predictive of altered responsivity to internal or external stimuli promoting behavioral responses. For example, the “hate circuit” might lose its coherency in the patients in a resting state, but regain this coherency and function normally in response to appropriate stimuli. This is certainly an issue for all resting state studies requiring further investigation although, as we will discuss below, there are some in-

teresting parallels between our current findings and previous studies showing stimulus-evoked changes in these same circuits in depressed patients.

So what might be the significance of the uncoupling we have found bilaterally in the so called “hate circuit” of depressed patients? This circuit is associated with feelings of hate because it has been reported that the superior frontal gyrus, insula and putamen are the three main brain regions showing altered activation when individuals view people who they hate (16), although interestingly they are also affected similarly by seeing people you love, or have loved but recently been rejected by (16, 26-28). The insula region is also reported to be involved in feelings of disgust as well as other emotions (29) and a recent fMRI study has shown enhanced responses in the insula to faces expressing disgust (30). A relationship between the different components of the “hate circuit” and various psychiatric and neurodegenerative diseases such as schizophrenia (31), Huntington’s disease (32, 33) and depression (30) has already been reported.

A recent meta-analysis of changes in brain activation during depression shows that the superior frontal gyrus, insula and putamen are consistently affected (34). This meta-analysis reports that the superior frontal gyrus shows increased activation in depressed patients as well as enhanced activation in response to positive emotional stimuli and decreased

activation in response to negative emotional stimuli. The insula exhibits decreased basal activity and responses to both positive and negative emotional stimuli in depressed patients. The putamen on the other hand shows decreased responses to positive emotional stimuli and increased ones to negative emotional stimuli. The differential patterns of changes in these three structures are consistent with our finding that in depressed patients they have become functionally uncoupled both in the resting state and during exposure to emotional stimuli, although the latter needs to be confirmed in further experiments. Interestingly the meta-analysis also reports that with SSRI treatments all three structures tend to show decreased activity which might suggest re-establishment of the coupling between them leads to more co-ordination between them.

Depression is associated with reduced size of the putamen (35), although we did not find any evidence for this in our depressed patients. Elevated dopamine D2 receptor binding (36) and increased oxidative stress (37) have also been reported in the putamen of depressed patients, and stroke patients with damage to this region can show depressive symptoms (38). Altered functioning of the insular cortex has been found in a number of psychiatric disorders, including depression (39). Depression is associated with a disturbed sense of interoceptive awareness and the insula appears to be important in this respect (40). The superior frontal gyrus has also been reported to be reduced in size in depressed pa-

tients (41) although we did not find this in our patients.

Depression is often characterized by intense self loathing and while it is associated with anhedonia there is no obvious indication that depressives are less prone to hate others. One possibility is that the uncoupling of this circuit could be associated with impaired ability to control and learn from social or other situations which provoke feelings of hate towards self or others. This in turn could lead to an inability to deal appropriately with feelings of hate and an increased likelihood of both uncontrolled self-loathing and withdrawal from social interactions. Depressed patients also have problems in controlling negative thoughts and so a potential hypothesis is that the functional uncoupling in this circuit may be contributing to impaired cognitive control over pervasive internal feelings of self-loathing or hatred towards others and/or external circumstances. Indeed, reduced cognitive control over emotions has been proposed as one of the important factors in depression (42).

The "hate circuit" may be involved in the control of other behaviors influenced by depression. The same brain regions, for example, also appear to be involved in feelings of self-awareness. A recent experiment using real-time fMRI training has reported that feedback enhanced metacognitive awareness, in terms of turning attention towards or away from their own thoughts, results in increased activation of the prefrontal cortex, insula and putamen (43). Depressed patients also have problems in con-

trolling their thoughts and perhaps feedback training on meta-cognitive awareness might actually be a potential therapeutic approach for restoring functional coupling in this circuit.

Other significantly affected circuits in depressed patients were those associated with risk and action, reward and emotion, attention and memory processing. The risk/action circuitry comprises the inferior frontal gyrus and its connections with the precentral gyrus in the left hemisphere and supramarginal gyrus in the right hemisphere. The inferior frontal gyrus is particularly associated with response inhibition (44, 45) and its activation has been found to be positively correlated with perception of and taking higher risks in a variety of experimental contexts (46-48). These pathways together with the left precentral gyrus connection to the inferior parietal lobe are all reduced in strength in depressed patients and are part of the "mirror" system involved in imitating the actions of others and also responding to self-movements (49, 50). They are also involved in aspects of semantic processing which can also be impaired in depressed patients (51). In this context it is interesting to note that connectivity between the angular gyrus and cuneus is weakened in our depressed patients which might contribute to impaired semantic processing (52). The inferior parietal lobe has also been shown to be important for the perception of emotions during presentation of facial stimuli (53). This finding, coupled with the observed weakening of connections between the fusiform and lingual

gyri provides a neural basis for impaired face emotion processing in depressed patients. Indeed, altered responsiveness to emotional facial stimuli in depressives has been taken as one of the biomarkers for early diagnosis (54).

A meta-analysis of brain regions affected in depressed patients has shown the inferior frontal gyrus to be influenced both in terms of basal activity and responses to affective stimuli (34). Overall therefore one possibility is that, as with the "hate circuit", the altered coupling in the risk/action circuit may also reflect reduced cognitive control via the frontal cortex over a range of adaptive responses to emotional stimuli.

The part of an emotion and reward circuit significantly altered in depressed patients comprises the links between the superior and medial regions of the orbitofrontal cortex, and is known to be closely related to psychiatric and developmental disorders such as schizophrenia (55), obsessive compulsive disorder (56) and autism (57). Neuroimaging studies have found that the reward value, the expected reward value, and even the subjective pleasantness of foods and other reinforcers are also represented in the orbitofrontal cortex (58, 59). Interestingly, there is a clear difference between the effects of depression on right and left brain hemispheres in relation to functional coupling in this pathway. Our results show that it is increased in strength in the right hemisphere and decreased in the left. There is evidence that the right orbitofrontal cortex is more activated by

punishment whereas the left is activated more by positive rewards (60). This may therefore possibly reflect increased responsivity to negative stimuli (right hemisphere) and decreased responses to positive stimuli (left) typically found in depressed patients. Since there are also strengthened connections between the right inferior frontal gyrus and the right inferior orbitofrontal cortex, and also the medial frontal gyrus in depressed patients in the attention circuit, this might also reflect an increased attentional bias towards negative stimuli.

Another main pathway affected in both groups of depressed patients was that between the hippocampus and parahippocampal gyrus. This may reflect aspects of impaired memory functions in depressed patients. Interestingly there is increasing evidence that neurogenesis in the hippocampus is important for learning and there may be a link between depression and reduced neurogenesis in the hippocampus (61, 62). Loss of hippocampal neurons is found in some depressive individuals and correlates with impaired memory and dysthymic mood. Anti-depressant drugs which increase serotonin levels in the brain may also help by stimulating neurogenesis and increasing the total mass of the hippocampus thereby helping to restore mood and memory dysfunction (63).

The main focus of this study was to identify functional pathways altered in both FEMDD and RMDD patients who were currently suffering from severe depression in order to try and help establish which ones are

most strongly linked with depression per se. There were clearly a large number of differences between the patient groups which emphasizes the importance of not basing analyses of potential brain correlates of depression on a single type of patient group. However, it must be emphasized that the RMDD group had only been drug-treatment free for 24 hours compared with at least 2 weeks for the FEMDD group and so some of the differences observed in the two groups could be drug related although obviously in the REMDD group their severe depression symptoms had not ameliorated significantly in response to these drugs. It is clear that it would need a more detailed investigation on drug-free patients in the two groups to establish which differences between the two patient groups could be of potential relevance. However, as already mentioned above, it is of particular interest at this stage that alterations in amygdala and cingulate connectivity, which have often been considered to be central to neural circuitry involved in depression, are different in these two patient groups despite both having similar current levels of severe depression.

Acknowledgements

S. Guo is supported by The National Natural Science Foundation of China (NSFC) (10901049) and excellent talent of Hunan Normal University (ET11001) and Key Laboratory of Computational and Stochastic Mathematics and Its Application of Hunan province (09K026). T. Ge is supported by the China Scholarship Council (CSC). Zhening Liu is supported by research grants from the NSFC (81071092), the National Basic Research Program of China (2007CB512300), and the 11th Five Year Key Pro-

gram for Science and Technology Development of China (2007BAI17B05). J. Feng is a Royal Society Wolfson Research Merit Award holder, partially supported by an EU grant BION, a UK EPSRC grant and National Centre for Mathematics and Interdisciplinary Sciences (NCMIS) in Chinese Academy of Sciences.

Conflict of interest

The authors declare no conflict of interest.

REFERENCES

1. Raichle M. The brain's dark energy. *Scientific American Magazine*. 2010; **302**(3): 44-9.
2. Zhang D, Raichle ME. Disease and the brain's dark energy. *Nature Reviews Neurology*. 2010; **6**(1): 15-28.
3. Zhang D, Snyder AZ, Fox MD, Sansbury MW, Shimony JS, Raichle ME. Intrinsic functional relations between human cerebral cortex and thalamus. *Journal of neurophysiology*. 2008; **100**(4): 1740.
4. Greicius MD, Flores BH, Menon V, Glover GH, Solvason HB, Kenna H*, et al.* Resting-state functional connectivity in major depression: abnormally increased contributions from subgenual cingulate cortex and thalamus. *Biological psychiatry*. 2007; **62**(5): 429-37.
5. Anand A, Li Y, Wang Y, Lowe MJ, Dzemidzic M. Resting state corticolimbic connectivity abnormalities in unmedicated bipolar disorder and unipolar depression. *Psychiatry Research: Neuroimaging*. 2009; **171**(3): 189-98.
6. Anand A, Li Y, Wang Y, Wu J, Gao S, Bukhari L*, et al.* Activity and connectivity of brain mood regulating circuit in depression: a functional magnetic resonance study. *Biological psychiatry*. 2005; **57**(10): 1079-88.
7. Anand A, Li Y, Wang Y, Wu J, Gao S, Bukhari L*, et al.* Antidepressant effect on connectivity of the mood-regulating circuit: an FMRI study. *Neuropsychopharmacology*. 2005; **30**(7): 1334-44.
8. Kiviniemi V, Kantola JH, Jauhiainen J, Hyvärinen A, Tervonen O. Independent component analysis of nondeterministic fMRI signal sources. *Neuroimage*. 2003; **19**(2): 253-60.
9. McKeown MJ, Makeig S, Brown GG, Jung TP, Kindermann SS, Bell AJ*, et al.* Analysis of fMRI data by blind separation into independent spatial components. *Human brain mapping*. 1998; **6**(3): 160-88.
10. Smith SM, Fox PT, Miller KL, Glahn DC, Fox PM, Mackay CE*, et al.* Correspondence of the brain's functional architecture during activation and rest. *Proceedings of the National Academy of Sciences*. 2009; **106**(31): 13040.
11. Greicius MD, Krasnow B, Reiss AL, Menon V. Functional connectivity in the resting brain: a network analysis of the default mode hypothesis. *Proceedings of the National Academy of Sciences*. 2003; **100**(1): 253.
12. Fox MD, Snyder AZ, Vincent JL, Corbetta M, Van Essen DC, Raichle ME. The human brain is intrinsically organized into dynamic, anticorrelated functional networks. *Proceedings of the National Academy of Sciences of the United States of America*. 2005; **102**(27): 9673.
13. Biswal B, Yetkin FZ, Haughton VM, Hyde JS. Functional connectivity in the motor cortex of resting human brain using echo-planar MRI. *Magnetic Resonance in Medicine*. 1995; **34**(4): 537-41.
14. Cole DM, Smith SM, Beckmann CF. Advances and pitfalls in the analysis and interpretation of resting-state FMRI data. *Frontiers in systems neuroscience*. 2010; **4**.
15. Yang B, Liu J, Feng J. On the Spectral Characterization and Scalable Mining of Network Communities. *Knowledge and Data Engineering, IEEE Transactions on*. (99): 1.
16. Zeki S, Romaya JP. Neural correlates of hate. *PLoS One*. 2008; **3**(10): e3556.
17. Hamilton M. A rating scale for depression. *Journal of neurology, neurosurgery, and psychiatry*. 1960; **23**(1): 56.
18. Miller IW, Bishop S, Norman WH, Maddever H. The modified Hamilton Rating Scale for Depression: reliability and validity. *Psychiatry Research*. 1985; **14**(2): 131-42.
19. Furtado CP, Maller JJ, Fitzgerald PB. A magnetic resonance imaging study of the entorhinal cortex

in treatment-resistant depression. *Psychiatry Research: Neuroimaging*. 2008; **163**(2): 133-42.
20. Shah PJ, Ebmeier KP, Glabus MF, Goodwin GM. Cortical grey matter reductions associated with treatment-resistant chronic unipolar depression. Controlled magnetic resonance imaging study. *The British journal of psychiatry*. 1998; **172**(6): 527.
21. Nierenberg A, Amsterdam J. Treatment-resistant depression: definition and treatment approaches. Discussion. *The Journal of clinical psychiatry*. 1990; **51**(6): 39-50.
22. Iidaka T, Nakajima T, Suzuki Y, Okazaki A, Maehara T, Shiraishi H. Quantitative regional cerebral blood flow measured by Tc-99m HMPAO SPECT in mood disorder. *Psychiatry Research: Neuroimaging*. 1997; **68**(2-3): 143-54.
23. Yan C, Zang Y. DPARSF: a MATLAB toolbox for "pipeline" data analysis of resting-state fMRI. *Frontiers in systems neuroscience*. 2010; **4**.
24. Tzourio-Mazoyer N, Landeau B, Papathanassiou D, Crivello F, Etard O, Delcroix N*, et al.* Automated anatomical labeling of activations in SPM using a macroscopic anatomical parcellation of the MNI MRI single-subject brain. *Neuroimage*. 2002; **15**(1): 273-89.
25. Biswal BB, Mennes M, Zuo XN, Gohel S, Kelly C, Smith SM*, et al.* Toward discovery science of human brain function. *Proceedings of the National Academy of Sciences*. 2010; **107**(10): 4734.
26. Bartels A, Zeki S. The neural basis of romantic love. *Neuroreport*. 2000; **11**(17): 3829.
27. Bartels A, Zeki S. The neural correlates of maternal and romantic love. *Neuroimage*. 2004; **21**(3): 1155-66.
28. Fisher HE, Brown LL, Aron A, Strong G, Mashek D. Reward, addiction, and emotion regulation systems associated with rejection in love. *Journal of neurophysiology*. 2010; **104**(1): 51.
29. Chen YH, Dammers J, Boers F, Leiberg S, Edgar JC, Roberts TPL*, et al.* The temporal dynamics of insula activity to disgust and happy facial expressions: A magnetoencephalography study. *Neuroimage*. 2009; **47**(4): 1921-8.
30. Surguladze SA, El-Hage W, Dalgleish T, Radua J, Gohier B, Phillips ML. Depression is associated with increased sensitivity to signals of disgust: A functional magnetic resonance imaging study. *Journal of psychiatric research*. 2010.
31. Wylie KP, Tregellas JR. The role of the insula in schizophrenia. *Schizophrenia research*. 2010; **123**(2-3): 93-104.
32. Calder AJ, Keane J, Manes F, Antoun N, Young AW. Impaired recognition and experience of disgust following brain injury. *Nature Neuroscience*. 2000; **3**(11): 1077-8.
33. Calder AJ, Lawrence AD, Young AW. Neuropsychology of fear and loathing. *Nature Reviews Neuroscience*. 2001; **2**(5): 352-63.
34. Fitzgerald PB, Laird AR, Maller J, Daskalakis ZJ. A meta analytic study of changes in brain activation in depression. *Human brain mapping*. 2008; **29**(6): 683-95.
35. Husain MM, McDonald WM, Doraiswamy PM, Figiel GS, Na C, Escalona PR*, et al.* A magnetic resonance imaging study of putamen nuclei in major depression. *Psychiatry Research: Neuroimaging*. 1991; **40**(2): 95-9.
36. Meyer JH, McNeely HE, Sagrati S, Boovariwala A, Martin K, Verhoeff N*, et al.* Elevated putamen D2 receptor binding potential in major depression with motor retardation: an [11C] raclopride positron emission tomography study. *American Journal of Psychiatry*. 2006; **163**(9): 1594.
37. Michel TM, Camara S, Tatschner T, Frangou S, Sheldrick AJ, Riederer P*, et al.* Increased xanthine oxidase in the thalamus and putamen in depression. *World Journal of Biological Psychiatry*. 2010; **11**(2_2): 314-20.

38. Vataja R, Leppavuori A, Pohjasvaara T, Mantyla R, Aronen HJ, Salonen O*, et al.* Poststroke depression and lesion location revisited. *Journal of Neuropsychiatry and Clinical Neurosciences*. 2004; **16**(2): 156.
39. Craig A. How do you feel—now? The anterior insula and human awareness. 2009.
40. Wiebking C, Bauer A, de GRECK M, Duncan NW, Tempelmann C, Northoff G. Abnormal body perception and neural activity in the insula in depression: An fMRI study of the depressed "material me". *World Journal of Biological Psychiatry*. 2010; (0): 1-12.
41. Leung KK, Lee T, Wong M, Li L, Yip P, Khong PL. Neural correlates of attention biases of people with major depressive disorder: a voxel-based morphometric study. *Psychological medicine*. 2009; **39**(07): 1097-106.
42. Ebmeier K, Rose E, Steele D. Cognitive impairment and fMRI in major depression. *Neurotoxicity research*. 2006; **10**(2): 87-92.
43. McCaig RG, Dixon M, Keramatian K, Liu I, Christoff K. Improved modulation of rostrolateral prefrontal cortex using real-time fMRI training and meta-cognitive awareness. *Neuroimage*. 2010.
44. Aron AR, Robbins TW, Poldrack RA. Inhibition and the right inferior frontal cortex. *Trends in Cognitive Sciences*. 2004; **8**(4): 170-7.
45. Swick D, Ashley V. Left inferior frontal gyrus is critical for response inhibition. *BMC neuroscience*. 2008; **9**(1): 102.
46. Christopoulos GI, Tobler PN, Bossaerts P, Dolan RJ, Schultz W. Neural correlates of value, risk, and risk aversion contributing to decision making under risk. *The Journal of Neuroscience*. 2009; **29**(40): 12574.
47. Knoch D, Gianotti LRR, Pascual-Leone A, Treyer V, Regard M, Hohmann M*, et al.* Disruption of right prefrontal cortex by low-frequency repetitive transcranial magnetic stimulation induces risk-taking behavior. *The Journal of Neuroscience*. 2006; **26**(24): 6469.
48. Fecteau S, Pascual-Leone A, Zald DH, Liguori P, Théoret H, Boggio PS*, et al.* Activation of prefrontal cortex by transcranial direct current stimulation reduces appetite for risk during ambiguous decision making. *The Journal of Neuroscience*. 2007; **27**(23): 6212.
49. Macuga KL, Frey SH. Selective responses in right inferior frontal and supramarginal gyri differentiate between observed movements of oneself vs. another. *Neuropsychologia*. 2011.
50. Rizzolatti G, Sinigaglia C. The functional role of the parieto-frontal mirror circuit: interpretations and misinterpretations. *Nat Rev Neurosci*. 2010; **11**(4): 264-74.
51. Klumpp H, Deldin P. Review of brain functioning in depression for semantic processing and verbal fluency. *International Journal of Psychophysiology*. 2010; **75**(2): 77-85.
52. Démonet JF, Price C, Wise R, Frackowiak R. Differential activation of right and left posterior sylvian regions by semantic and phonological tasks: a positron-emission tomography study in normal human subjects. *Neuroscience letters*. 1994; **182**(1): 25-8.
53. Peeters R, Simone L, Nelissen K, Fabbri-Destro M, Vanduffel W, Rizzolatti G*, et al.* The representation of tool use in humans and monkeys: common and uniquely human features. *The Journal of Neuroscience*. 2009; **29**(37): 11523.
54. Hahn T, Marquand A, Ehlis A, Dresler T, Kittel-Schneider S, Jarczok T*, et al.* Integrating Neurobiological Markers of Depression. *Archives of general psychiatry*. 2010.
55. Larquet M, Coricelli G, Opolczynski G, Thibaut F. Impaired decision making in schizophrenia and orbitofrontal cortex lesion patients. *Schizophrenia research*. 2010; **116**(2-3): 266-73.
56. Chamberlain SR, Menzies L, Hampshire A, Suckling J, Fineberg NA, del Campo N*, et al.*

Orbitofrontal dysfunction in patients with obsessive-compulsive disorder and their unaffected relatives. *Science*. 2008; **321**(5887): 421.
57. Bachevalier J, Loveland KA. The orbitofrontal-amygdala circuit and self-regulation of social-emotional behavior in autism. *Neuroscience & Biobehavioral Reviews*. 2006; **30**(1): 97-117.
58. Kringelbach ML, Rolls ET. The functional neuroanatomy of the human orbitofrontal cortex: evidence from neuroimaging and neuropsychology. *Progress in neurobiology*. 2004; **72**(5): 341-72.
59. Rolls E, Hornak J, Wade D, McGrath J. Emotion-related learning in patients with social and emotional changes associated with frontal lobe damage. *Journal of Neurology, Neurosurgery & Psychiatry*. 1994; **57**(12): 1518.
60. O'Doherty J, Kringelbach ML, Rolls ET, Hornak J, Andrews C. Abstract reward and punishment representations in the human orbitofrontal cortex. *Nature Neuroscience*. 2001; **4**(1): 95-102.
61. Minkel J. Brain pathway may underlie depression: A crescent of electrical activity spotted in rats may allow researchers to map the depressed brain. *Scientific American Mind News, http://www.sciam.com/article.cfm*. 2007.
62. Airan RD, Meltzer LA, Roy M, Gong Y, Chen H, Deisseroth K. High-speed imaging reveals neurophysiological links to behavior in an animal model of depression. *Science*. 2007; **317**(5839): 819.
63. Becker S, Wojtowicz JM. A model of hippocampal neurogenesis in memory and mood disorders. *Trends in Cognitive Sciences*. 2007; **11**(2): 70-6.

Regions	Abbr.	Regions	Abbr.
Amygdala	AMYG	Orbitofrontal cortex (middle)	ORBmid
Angular gyrus	ANG	Orbitofrontal cortex (superior)	ORBsup
Anterior cingulate gyrus	ACG	Pallidum	PAL
Calcarine cortex	CAL	Paracentral lobule	PCL
Caudate	CAU	Parahippocampal gyrus	PHG
Cuneus	CUN	Postcentral gyrus	PoCG
Fusiform gyrus	FFG	Posterior cingulate gyrus	PCG
Heschl gyrus	HES	Precentral gyrus	PreCG
Hippocampus	HIP	Precuneus	PCUN
Inferior occipital gyrus	IOG	Putamen	PUT
Inferior frontal gyrus (opercula)	IFGoperc	Rectus gyrus	REC
Inferior frontal gyrus (triangular)	IFGtriang	Rolandic operculum	ROL
Inferior parietal lobule	IPL	Superior occipital gyrus	SOG
Inferior temporal gyrus	ITG	Superior frontal gyrus (dorsal)	SFGdor
Insula	INS	Superior frontal gyrus (medial)	SFGmed
Lingual gyrus	LING	Superior parietal gyrus	SPG
Middle cingulate gyrus	MCG	Superior temporal gyrus	STG
Middle occipital gyrus	MOG	Supplementary motor area	SMA
Middle frontal gyrus	MFG	Supramarginal gyrus	SMG
Middle temporal gyrus	MTG	Temporal pole (middle)	TPOmid
Olfactory	OLF	Temporal pole (superior)	TPOsup
Orbitofrontal cortex (inferior)	ORBinf	Thalamus	THA
Orbitofrontal cortex (medial)	ORBmed		

Table 1: The names and abbreviations of the regions of interest (ROIs).

Figure Legends

Figure 1 a. Community structure of the normal template. b. The correlation coefficient matrix of the BOLD signals from 90 ROIs of one randomly selected subject. c. (Left) Medial view of the surface of the brain. (Right) The lateral view of the surface of the brain. Different colors represent different communities.

Figure 2 a. Bar plot of the scores of the FEMDD network compared with the normal template. b. Bar plot of the scores of the FEMDD network compared with the normal template. In both a and b, red bars represent the links appeared in patients' network while disappeared in normal template, blue bars are vise verse. c. Summarized scores for the six communities.

Figure 3 a. Functional network structure with different links of normal template and FEMDD patients. b. Functional network structure with different links of normal template and RMDD patients. In both a and b, red lines are links which appear in depression network only while blue lines are links which appear in normal template only. The widths of the lines are proportional to the scores.

Figure 4 a. The common links of the FEMDD and RMDD networks. b. Different links of the FEMDD and RMDD networks. In both a and b, red lines are links appear in depression network only while blue lines are links appear in normal template only. The widths of the lines are proportional to the scores.

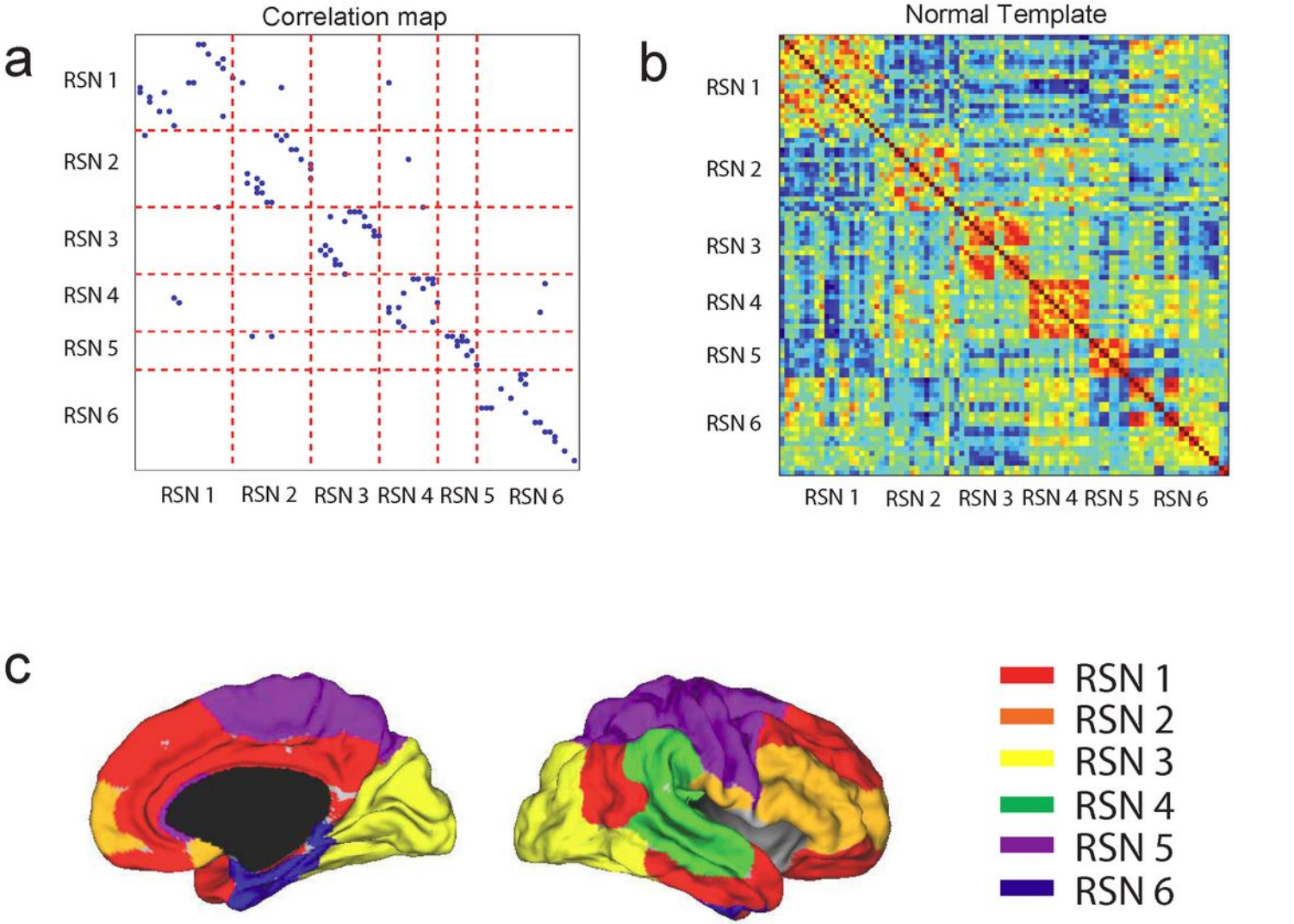
a
Correlation map
RSN 1
RSN 2
RSN 3
RSN 4
RSN 5
RSN 6
RSN 1 RSN 2 RSN 3 RSN 4 RSN 5 RSN 6
b
Normal Template
RSN 1
RSN 2
RSN 3
RSN 4
RSN 5
RSN 6
RSN 1 RSN 2 RSN 3 RSN 4 RSN 5 RSN 6
c
RSN 1
RSN 2
RSN 3
RSN 4
RSN 5
RSN 6

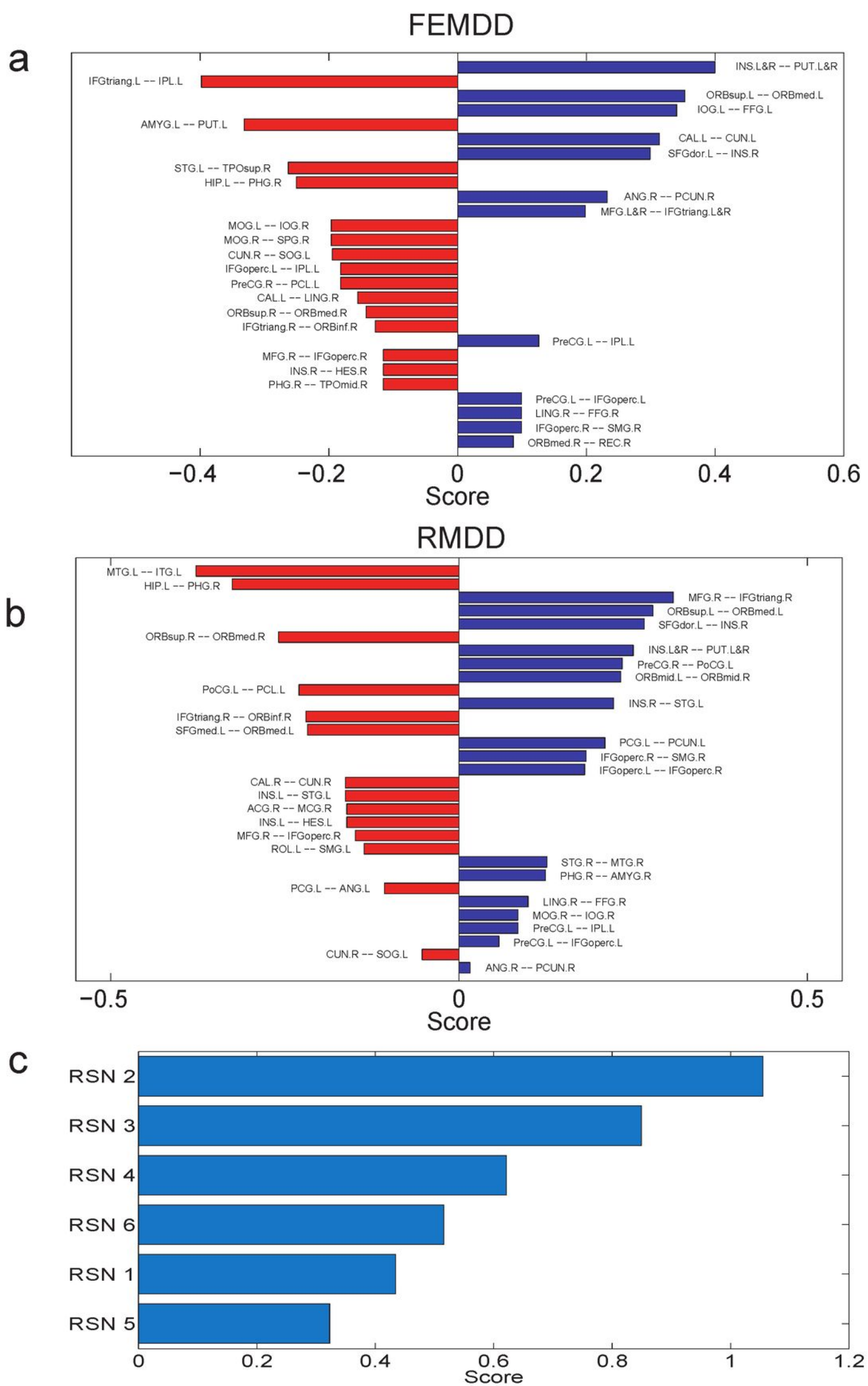
FEMDD
a
INS.L&R -- PUT.L&R
IFGtriang.L -- IPL.L
ORBsup.L -- ORBmed.L
IOG.L -- FFG.L
AMYG.L -- PUT.L
CAL.L -- CUN.L
SFGdor.L -- INS.R
STG.L -- TPOsup.R
HIP.L -- PHG.R
ANG.R -- PCUN.R
MFG.L&R -- IFGtriang.L&R
MOG.L -- IOG.R
MOG.R -- SPG.R
CUN.R -- SOG.L
IFGoperc.L -- IPL.L
PreCG.R -- PCL.L
CAL.L -- LING.R
ORBsup.R -- ORBmed.R
IFGtriang.R -- ORBinf.R
PreCG.L -- IPL.L
MFG.R -- IFGoperc.R
INS.R -- HES.R
PHG.R -- TPOmid.R
PreCG.L -- IFGoperc.L
LING.R -- FFG.R
IFGoperc.R -- SMG.R
ORBmed.R -- REC.R
−0.4
−0.2
0
0.2
0.4
0.6
Score
RMDD
b
MTG.L -- ITG.L
HIP.L -- PHG.R
MFG.R -- IFGtriang.R
ORBsup.L -- ORBmed.L
SFGdor.L -- INS.R
ORBsup.R -- ORBmed.R
INS.L&R -- PUT.L&R
PreCG.R -- PoCG.L
ORBmid.L -- ORBmid.R
PoCG.L -- PCL.L
INS.R -- STG.L
IFGtriang.R -- ORBinf.R
SFGmed.L -- ORBmed.L
PCG.L -- PCUN.L
IFGoperc.R -- SMG.R
IFGoperc.L -- IFGoperc.R
CAL.R -- CUN.R
INS.L -- STG.L
ACG.R -- MCG.R
INS.L -- HES.L
MFG.R -- IFGoperc.R
ROL.L -- SMG.L
STG.R -- MTG.R
PHG.R -- AMYG.R
PCG.L -- ANG.L
LING.R -- FFG.R
MOG.R -- IOG.R
PreCG.L -- IPL.L
PreCG.L -- IFGoperc.L
CUN.R -- SOG.L
ANG.R -- PCUN.R
−0.5
0
0.5
Score
c
RSN 2
RSN 3
RSN 4
RSN 6
RSN 1
RSN 5
0
0.2
0.4
0.6
0.8
1
1.2
Score

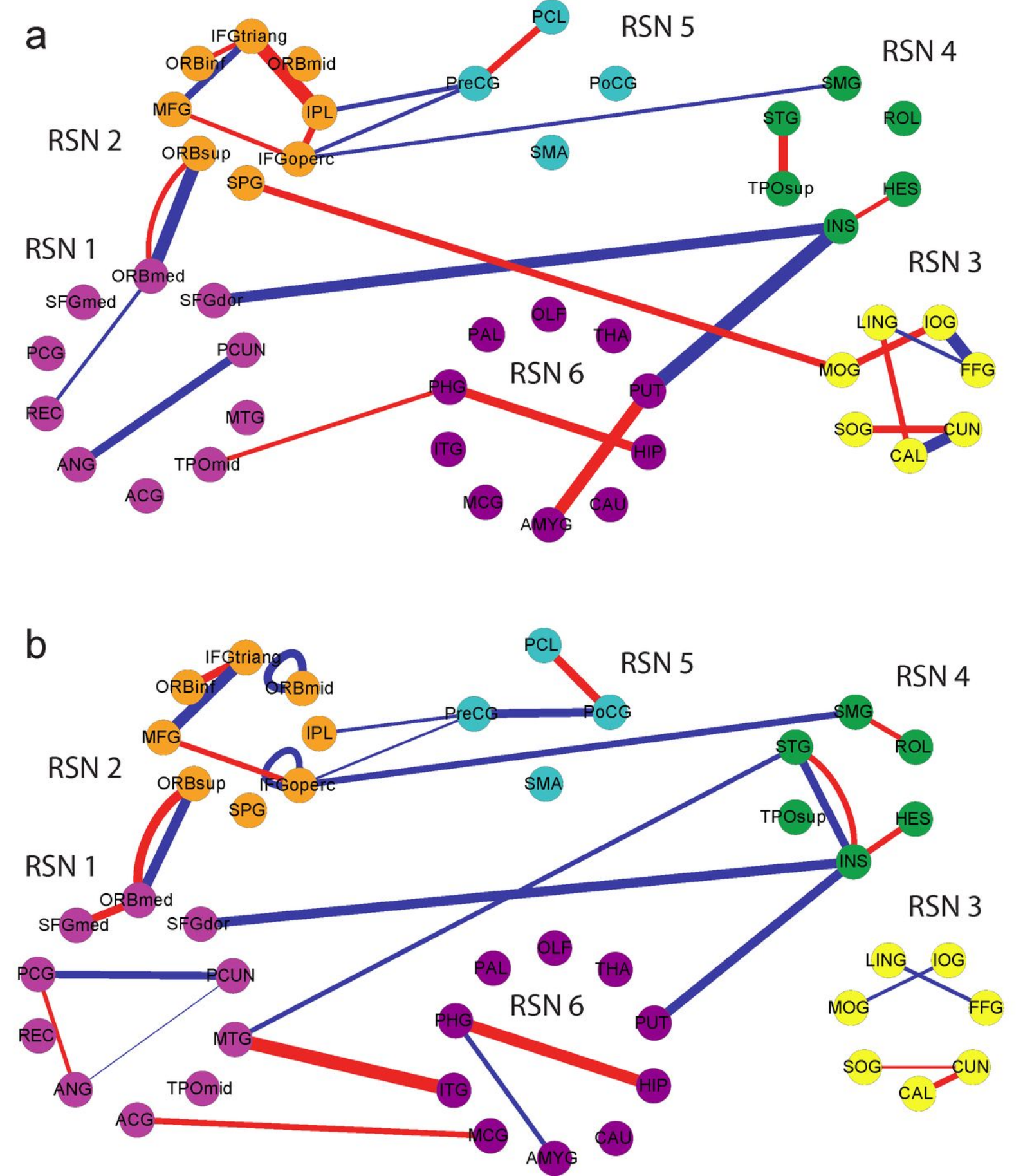
a
RSN 1
RSN 2
RSN 3
RSN 4
RSN 5
RSN 6
IFGtriang
ORBinf
ORBmid
MFG
IPL
PreCG
PCL
PoCG
SMG
STG
ROL
SMA
TPOsup
HES
ORBsup
IFGoperc
SPG
INS
ORBmed
SFGmed
SFGdor
OLF
PAL
THA
LING
IOG
MOG
FFG
PCG
PCUN
PHG
PUT
SOG
CUN
CAL
REC
MTG
ITG
HIP
ANG
TPOmid
ACG
MCG
CAU
AMYG
b
RSN 1
RSN 2
RSN 3
RSN 4
RSN 5
RSN 6
IFGtriang
ORBinf
ORBmid
MFG
IPL
PreCG
PCL
PoCG
SMG
ROL
STG
SMA
TPOsup
HES
ORBsup
IFGoperc
SPG
INS
ORBmed
SFGmed
SFGdor
OLF
PAL
THA
LING
IOG
MOG
FFG
PCG
PCUN
PHG
PUT
SOG
CUN
CAL
REC
MTG
ITG
HIP
ANG
TPOmid
ACG
MCG
CAU
AMYG

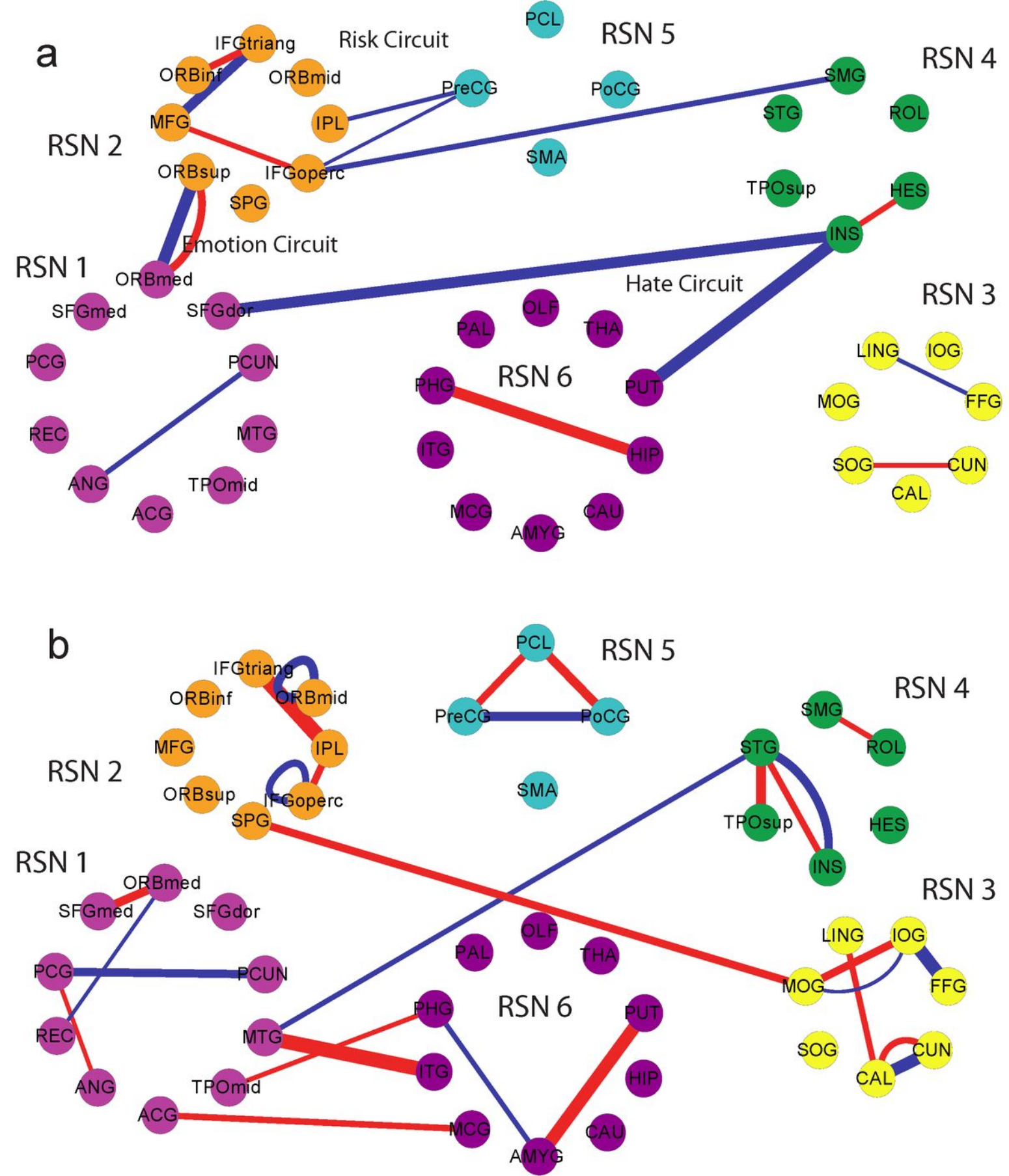
a
Risk Circuit
Emotion Circuit
Hate Circuit
RSN 1
RSN 2
RSN 3
RSN 4
RSN 5
RSN 6
IFGtriang
ORBinf
ORBmid
MFG
IPL
PreCG
PCL
PoCG
SMG
STG
ROL
SMA
ORBsup
IFGoperc
SPG
TPOsup
HES
INS
ORBmed
SFGmed
SFGdor
OLF
PAL
THA
PUT
PHG
HIP
PCG
PCUN
REC
MTG
ITG
ANG
TPOmid
ACG
MCG
AMYG
CAU
LING
IOG
MOG
FFG
SOG
CUN
CAL
b
IFGtriang
ORBinf
ORBmid
MFG
IPL
ORBsup
IFGoperc
SPG
PCL
PreCG
PoCG
SMA
SMG
ROL
STG
TPOsup
HES
INS
ORBmed
SFGmed
SFGdor
PCG
PCUN
REC
ANG
ACG
OLF
PAL
THA
PHG
PUT
MTG
ITG
TPOmid
HIP
MCG
AMYG
CAU
LING
IOG
MOG
FFG
SOG
CUN
CAL